

UNIVERSIDADE ESTADUAL DE CAMPINAS  
SISTEMA DE BIBLIOTECAS DA UNICAMP  
REPOSITÓRIO DA PRODUÇÃO CIENTÍFICA E INTELLECTUAL DA UNICAMP

**Versão do arquivo anexado / Version of attached file:**

Versão do Editor / Published Version

**Mais informações no site da editora / Further information on publisher's website:**

<https://onlinelibrary.wiley.com/doi/abs/10.1002/mop.30196>

**DOI: 10.1002/mop.30196**

**Direitos autorais / Publisher's copyright statement:**

©2016 by John Wiley & Sons. All rights reserved.

DIRETORIA DE TRATAMENTO DA INFORMAÇÃO

Cidade Universitária Zeferino Vaz Barão Geraldo

CEP 13083-970 – Campinas SP

Fone: (19) 3521-6493

<http://www.repositorio.unicamp.br>

6. D.C. Niu, C. Shan, T. Yuan, T.W. Huang, H.J. Lee, and C.Y. Chang, An X-band front-end module using HTS technique for a commercial dual mode radar, *IEEE Trans Appl Supercond* 15 (2005), 1008–1011.
7. R.J. Cameron and M. Yu, Design of manifold-coupled multiplexers, *IEEE Microw Mag* 8 (2007), 46–59.
8. Z.J. Shang, X.B. Guo, B.S. Cao, X.P. Zhang, B. Wei, Y. Heng, X.K. Song, G.N. Suo, J.C. Wang, and Q.R. Li, Design and performance of an HTS wideband microstrip bandpass filter at X-band, *Microw Opt Technol Lett* 55 (2013), 1027–1029.
9. X.K. Song, B. Wei, B.S. Cao, X.P. Zhang, X.B. Guo, G.Y. Zhang, and X. Zhan, High performance narrowband superconducting filters with high Q values at X-band without tuning, *Microw Opt Technol Lett* 56 (2014), 1516–1520.
10. T.N. Zheng, X.B. Guo, B.S. Cao, B. Wei, X.P. Zhang, C. Feng, and G.Y. Zhang, Design of compact superconducting diplexer with spiral short-circuited stubs, *IEEE Trans Appl Supercond* 24 (2014), 1500405.
11. Y. Heng, X.B. Guo, B.S. Cao, B. Wei, X.P. Zhang, G.Y. Zhang, and X.K. Song, A narrowband superconducting quadruplexer with high isolation, *IEEE Trans Appl Supercond* 24 (2014), 1500506.
12. J.-S. Hong, *Microstrip filters for RF/microwave applications* second edition, Wiley, New York, 2011, p. 73.

© 2016 Wiley Periodicals, Inc.

## PERFORMANCE IMPROVEMENT OF CASCADED DISPERSION COMPENSATION BASED FIBER BRAGG GRATINGS BY SMART SELECTION

Elias Giacomidis,<sup>1</sup> Andreas Perentos,<sup>2</sup> and Ivan Aldaya<sup>3</sup>

<sup>1</sup> Centre of Ultra High Bandwidth for Optical Systems (CUDOS) and Institute of Photonics Systems Optical Science (IPOS), University of Sydney, Physics Road, Sydney, NSW 2006, Australia; Corresponding author: e.giacomidis@physics.usyd.edu.au

<sup>2</sup> Department of Electrical and Computer Engineering, University of Cyprus, Cyprus

<sup>3</sup> Physics Institute, State University of Campinas, Campinas 777, Brazil

Received 4 May 2016

**ABSTRACT:** A Monte-Carlo (MC)-based heuristic algorithm is applied, for the first time, in cascaded chromatic dispersion compensation based fiber Bragg gratings (FBGs) for performance improvement by means of group delay ripple mitigation. It is shown that the MC method outperforms random FBG selection by 37.5% and 35% for 10 and 15 cascaded FBGs, respectively. © 2016 Wiley Periodicals, Inc. *Microwave Opt Technol Lett* 58:2954–2957, 2016; View this article online at [wileyonlinelibrary.com](http://wileyonlinelibrary.com). DOI 10.1002/mop.30196

**Key words:** Fiber Bragg Gratings; Monte Carlo algorithm; Group Delay Ripple

### 1. INTRODUCTION

Fiber Bragg gratings (FBGs) are widely used in optical communications due to the flexibility of customizing both the amplitude and phase of the frequency response. FBGs have a large variety of applications, such as in fiber-ring lasers as frequency selective mechanism [1], microwave photonics [2], and wavelength-division multiplexing (WDM) for compensating fiber chromatic dispersion (CD). Compared with CD compensating fibers, FBG-based CD modules are more compact, have lower insertion losses, induce less nonlinear distortion and can be designed to compensate both 1st- and 2nd-order CD [3]. Given the importance of the high accumulated CD in optical long-

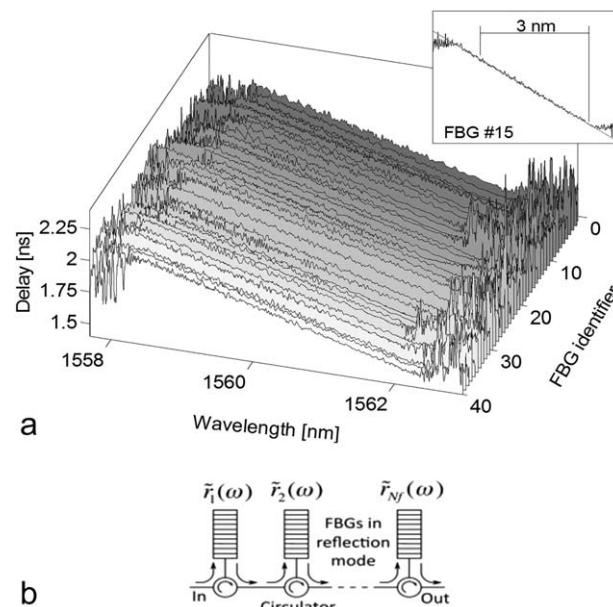


**Figure 1** (a) GD of 40 dispersion compensating FBGs. Inset: GD for one of the filters (FBG #15). (b) Concatenation of  $N_F$  FBGs in reflective mode

haul links, FBGs of several meters are required. As the FBG length increases, it is difficult to keep the grating period constant during the fabrication process resulting in phase discontinuities. Consequently, long FBGs introduce large GDR, i.e. the deviation of the group delay (GD) from its nominal value, as depicted in Figure 1(a) and its inset. The impact of GDR on the signal quality has been investigated in Ref. [3], concluding that it should be minimized as it deteriorates the optical link performance, especially for high bit-rate transmission. Since long FBGs are likely to suffer from considerable phase discontinuities it would be advantageous to replace them with a number of shorter FBGs. A cascaded configuration could be implemented either in transmission or reflection mode, as shown in Figure 1(b). Operating in transmission mode results in resonance induced frequency fading. On the other hand, reflection mode operation suffers from accumulated insertion loss of the required circulators. However, with the advection of low-loss circulators (0.44 dB) [4], cascading a relatively high number of FBGs is feasible. Typically, FBGs in a cascade configuration are chosen randomly from a pool of fabricated gratings. Due to variations in the fabrication process, some FBGs present lower GDR than others, thus by selecting the FBGs with the best individual GDR, the ratio of the total standard deviation in GDR to the individual FBG compensation length ( $\sigma_{\text{GDR}}/S$ ) could be reduced. However, it is not clear whether this approach results in the optimum  $\sigma_{\text{GDR}}/S$ .

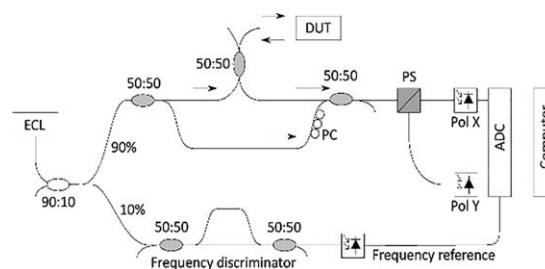


**Figure 2** Experimental setup for complex reflectivity of FBGs

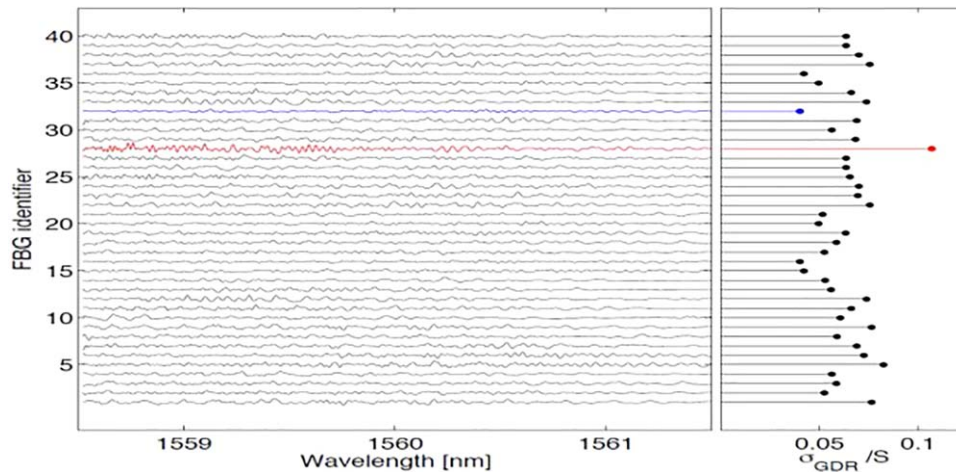


**Figure 3** Measured  $\sigma_{\text{GDR}}/S$  ratio for 40 FBGs, relative ripple-amplitude for the best (blue) and worst (red) FBGs in the set. [Color figure can be viewed at [wileyonlinelibrary.com](http://wileyonlinelibrary.com)]

In this paper, a novel technique is proposed for minimizing the total  $\sigma_{\text{GDR}}/S$  by combining a number of FBGs without the requirement of selecting the best GDRs out of the available FBG pool. The method consists of two steps (i) experimental characterization of the FBGs' phase responses using the optical frequency domain reflectometry (OFDR) technique and (ii) derivation of an optimized cascaded combination of the characterized FBGs. Due to the high number of possible combinations, testing each combination is not feasible, hence a heuristic approach must be considered. A Monte-Carlo (MC)-based optimization approach is adopted in this work. For the analysis of our method we employed 40 CD compensating FBGs. Results reveal that by optimal selection, the GDR of 20 cascaded FBGs is significantly reduced compared with random selection, whereas by selection of FBGs with optimum individual GDR, a smaller reduction is achieved.

## 2. EXPERIMENTAL SETUP AND MC APPLICATION

Forty raised-cosine-apodized FBGs of 1.5 mm length were characterized using a Mach-Zehnder interferometer (MZI) setup. The aforementioned FBGs were designed to compensate the 1st-order CD in the 1550 nm window, covering a frequency bandwidth of  $\sim 400$  GHz (3 nm). For each FBG, the GDR was measured using the OFDR technique, whose setup is outlined in Figure 2. An external cavity laser (ECL) was used as a tuneable light source. To have a frequency reference, 10% of the light

signal was passed through an MZI that acted as a frequency discriminator. The remaining 90% was sent to another interferometer where the device-under-test (DUT) was placed in one of its arms. A polarization controller (PC) was used to ensure that the optical fields at the ends of both arms had the same state of polarization. Afterwards, a polarization splitter (PS) segregated the X and Y polarizations, allowing characterization of the FBGs across both polarizations. Each polarization was detected using a separate photodetector (PD), while the frequency reference was detected using another PD. The received photocurrents were digitized using an analog-to-digital converter (ADC) before being processed in a computer, in which the complex reflectivity was calculated for each frequency/wavelength as an average value of the two polarizations.

The optimum selection of  $N_f$  FBGs out of a pool of  $N$  FBGs is a combinatorial optimization problem. For either low or high  $N_f$  values, the complexity is reasonable, but for  $N_f \rightarrow N/2$  the number of combinations is intractable: in the order of  $10^{11}$  for a pool of 40 FBGs,  $10^{14}$  for a pool of 50 FBGs, and  $10^{17}$  for a pool of 60 FBGs. For such high numbers of combinations, an extensive search is not feasible. A heuristic optimization approach, such as the MC, can provide an optimal solution in a relatively short period of time with low computational load. The MC optimization is based on the selection of the best solution from a random selection of samples; in this case FBGs. MC has been applied to several combinatorial problems due to its

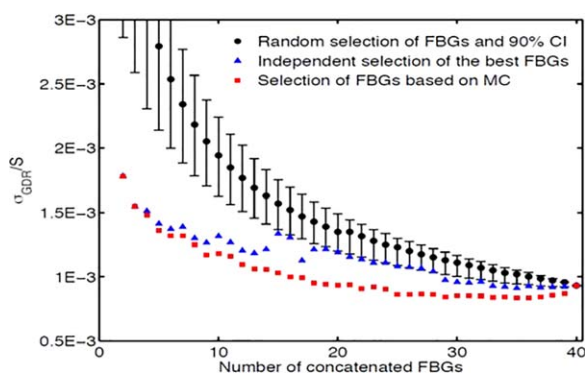


**Figure 4** Cascaded  $\sigma_{\text{GDR}}/S$  ratio for random selection, independent selection, and optimal selection using MC. [Color figure can be viewed at [wileyonlinelibrary.com](http://wileyonlinelibrary.com)]

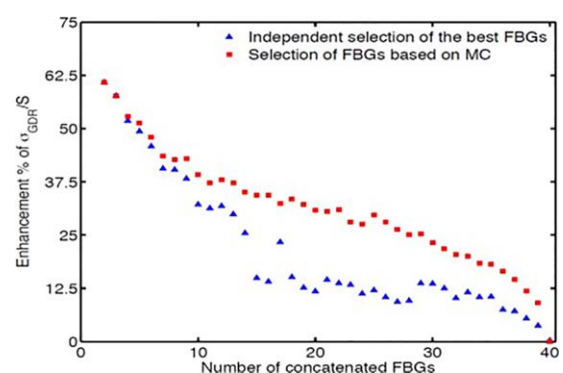


**Figure 5** Average enhancement percentage with individual selection of best FBGs and with optimal selection using MC. [Color figure can be viewed at [wileyonlinelibrary.com](http://wileyonlinelibrary.com)]

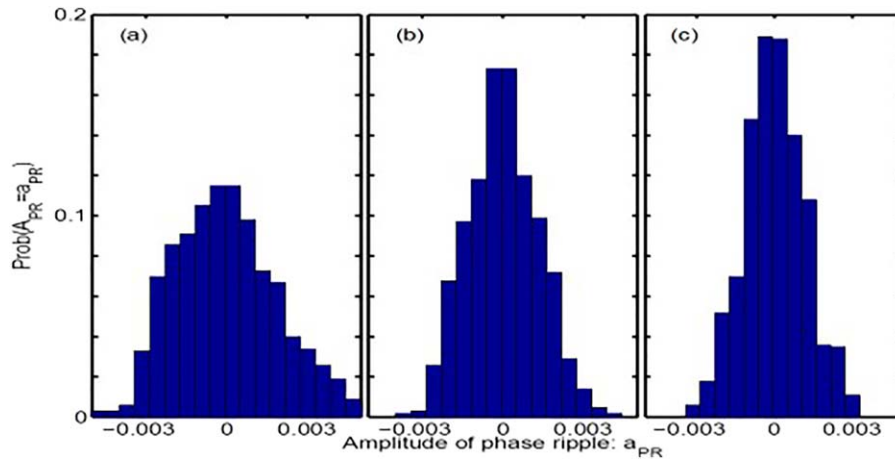


**Figure 6** Histograms of the phase ripple amplitude of 20 FBGs: (a) random, (b) individual, and (c) MC. [Color figure can be viewed at [wileyonlinelibrary.com](http://wileyonlinelibrary.com)]

simplicity and efficiency [5]. When the number of tested samples is high enough, the optimum solution is approximated.

In comparison with state-of-the-art heuristic methods (e.g., Ant Colony [6]), the MC is easier to code especially in its basic form, considering uniform sampling. More sophisticated MC implementations, such as the likelihood weighting, improves the convergence speed, which however, it is out of the scope of this work. It is worth noting that even if the MC algorithm is efficient enough to obtain acceptable results for 40 FBGs, for a larger number of combinations (i.e., more filters in the pool) a more powerful optimization algorithm may be required. Figure 3 illustrates the experimentally obtained GDR and the measured  $\sigma_{\text{GDR}}/S$  for each FBG (the worst FBG in terms of its GDR is highlighted in red, whereas the best one is highlighted in blue). The high variance of the  $\sigma_{\text{GDR}}/S$  ratio can be attributed to fabrication tolerances. In Figure 4, the  $\sigma_{\text{GDR}}/S$  ratios of  $N_f$  cascaded FBGs are shown for three cases (i) random selection of FBGs, (ii) individual selection of the best FBGs, and (iii) optimal selection using the MC method. For case (i), the average and the 90% confidence interval (CI) are presented to show the amount of CD among the randomly selected combinations. The monotonic decreasing tendency of the average  $\sigma_{\text{GDR}}/S$  of  $N_f$  randomly selected cascaded FBGs decays proportionally to  $N_f - 1/2$ .

In the same manner, the variance of  $\sigma_{\text{GDR}}/S$  decreases because the weight of each FBG decreases with an increment in  $N_f$ , and additionally, the average value is shifted from the center of the CI. The latter occurs due to the asymmetry in the resulting GDR distribution (close to a Rayleigh distribution). The selections obtained through individual selection and the MC, outperform the random selection for the whole range of  $N_f$  (except when  $N_f = N$ , where only 1 possible combination exists). Both combinations are out of the 90% CI, therefore, it is unlikely to achieve a performance similar to the one achieved with individual selection or MC by randomly selecting the FBGs. For a low number of cascaded stages, i.e.  $<10$ , individual selection and MC-selection result in similar performances. This happens due to the low number of cascaded FBGs, resulting in a restriction of the number of combination/selection where the GDRs are mutually compensated. As the number of stages increases, the chance to find a combination in which the GDR is fully compensated is higher.

According to Figures (4 and 5), the  $\sigma_{\text{GDR}}/S$  enhancement of individual best FBGs selection and MC-based-selection, are

more significant for low number of cascaded filters. Compared with MC-selection, individual selection of the best FBGs is less robust in the sense that it presents higher variations as the number of stages increases. This can be attributed to the fact that MC-selection considers the optimum value of a great number of combinations, whereas best individual selection considers only 1 combination, and, consequently is affected much more by the random nature of the samples. In Figure 5, it is also shown that the difference between individual selection and MC-selection enhancement is more evident between 10 and 25 stages. This can be explained by the higher number of combinations: the probability of finding a combination where the  $\sigma_{\text{GDR}}/S$  is reduced with respect to individual selection. For 10 cascaded FBGs, the  $\sigma_{\text{GDR}}/S$  ratio decreases on average by up to 35% and 37.5% using independent and MC, respectively. For 15 cascaded FBGs, this difference is considerably higher: 12.5% for independent selection and 35% for MC. Figure 6 presents the estimation of probability density functions based on the histograms of the ripple amplitude for 20 cascaded FBGs with (a) random selection, (b) individual selection of the best FBGs, and (c) MC. The narrower shape of the selection achieved by MC, confirms the fact that high amplitude peaks are cancelled out.

### 3. CONCLUSION

A novel method to reduce the  $\sigma_{\text{GDR}}/S$  ratio in cascaded CD compensating FBGs was proposed based on the characterization of a number of FBGs and a heuristic algorithm to find a set with reduced accumulated GDR. Results revealed that the proposed method outperforms previous approaches based on random selection and selection of the best individual FBGs. Significant improvements of 37.5% and 35% with respect to random selection were found for 10 and 15 cascaded FBGs, respectively. Selection of best individual FBGs results in 35% and 12.8% for the same number of cascaded FBGs. It is envisaged this work to play a dominant role in long-haul links where low GDR will reduce filter concatenation effects enabling system performance enhancement.

### ACKNOWLEDGMENTS

Centre of Excellence (CUDOS, CE110001018); FAPESP (2015/04113-0).

## REFERENCES

1. H. Liao, et al. Tunable and programmable fiber ring laser based on digital-controlled chirped fiber Bragg grating, *Front Optoelectron* 6 (2013), 468.
2. J. Capmany, et al. A tutorial on microwave photonic filters, *J Lightw Technol* 24 (2006), 201.
3. M. Filer et al., Estimation of phase ripple penalties for 40 Gb/s NRZ-DPSK Transmission, *Proc. OFC, NWD2*, San Diego, CA (2009).
4. Y. Makiuchi, et al. Development of a low-loss optical circulator, *Furukawa Rev* 22 (2002), 1.
5. S. Asmussen, *Stochastic simulations: Algorithm and analysis*, Ser: Stochastic Model Appl Probab 57 (2007).
6. M. Dorigo et al., *Ant colony optimization*, A Bradford Book, MIT Press, Cambridge, MA, 2004.

© 2016 Wiley Periodicals, Inc.

## LOW-PROFILE CIRCULARLY POLARIZED FABRY-PEROT CAVITY ANTENNA

Badreddine Ratni,<sup>1</sup> André de Lustrac,<sup>1,2</sup> Serge Villers,<sup>3</sup> and Shah Nawaz Burokur<sup>4</sup>

<sup>1</sup>IEF, CNRS, UMR 8622, Univ Paris Sud, Université Paris-Saclay, Orsay Cedex 91405, France

<sup>2</sup>Université Paris Ouest, Ville d'Avray 92410, France

<sup>3</sup>AIRBUS Defence and Space, Saint-Médard-en-Jalles 33165, France

<sup>4</sup>LEME, EA 4416, Université Paris Ouest, Ville d'Avray 92410, France; Corresponding author: sburokur@u-paris10.fr

Received 4 May 2016

**ABSTRACT:** The modeling and characterization of a low-profile circularly polarized directive antenna is reported. The proposed structure designed to operate near 2.1 GHz is evolved from a Fabry-Perot (FP) cavity with a patch antenna acting as the feed. One of the two reflectors is the antenna's ground plane and the other one is made from a bi-layered metamaterial-based partially reflecting surface (PRS) constituted by a capacitive and an inductive grid. The metasurface responds similarly to orthogonally polarized electric field. Calculations together with experimental results obtained from the fabricated prototype are presented. The results show a high directivity, low axial ratio and low level for the secondary lobes. © 2016 Wiley Periodicals, Inc. *Microwave Opt Technol Lett* 58:2957–2960, 2016; View this article online at [wileyonlinelibrary.com](http://wileyonlinelibrary.com). DOI 10.1002/mop.30195

**Key words:** metasurface; highly directive; Fabry-Perot (FP) cavity; microstrip patch antenna; circular polarization

## 1. INTRODUCTION

Nowadays, new generation of satellite communications systems require directive circularly polarized (CP) antennas. Classical method using an antenna array presents the main disadvantage of being bulky and requiring complex feeding network system to produce the circular polarization. An alternative interesting low-cost method consists in using a Fabry-Perot (FP) cavity antenna, originally introduced by Trentini [1]. The FP cavity antenna is composed of an embedded primary source between a partially reflective surface (PRS) and perfect electric conductor (PEC). Linearly polarized (LP) FP cavity antennas have been widely presented in literature [2–4] and have been validated for various functionalities such as beam steering [5–13] and frequency agility [14–16]. However, the CP versions have received less attention.

Several methods have been previously proposed for designing CP FP cavity antennas [17–23]. In Refs. [17] and [18], a CP FP cavity have been designed using a CP primary source and in

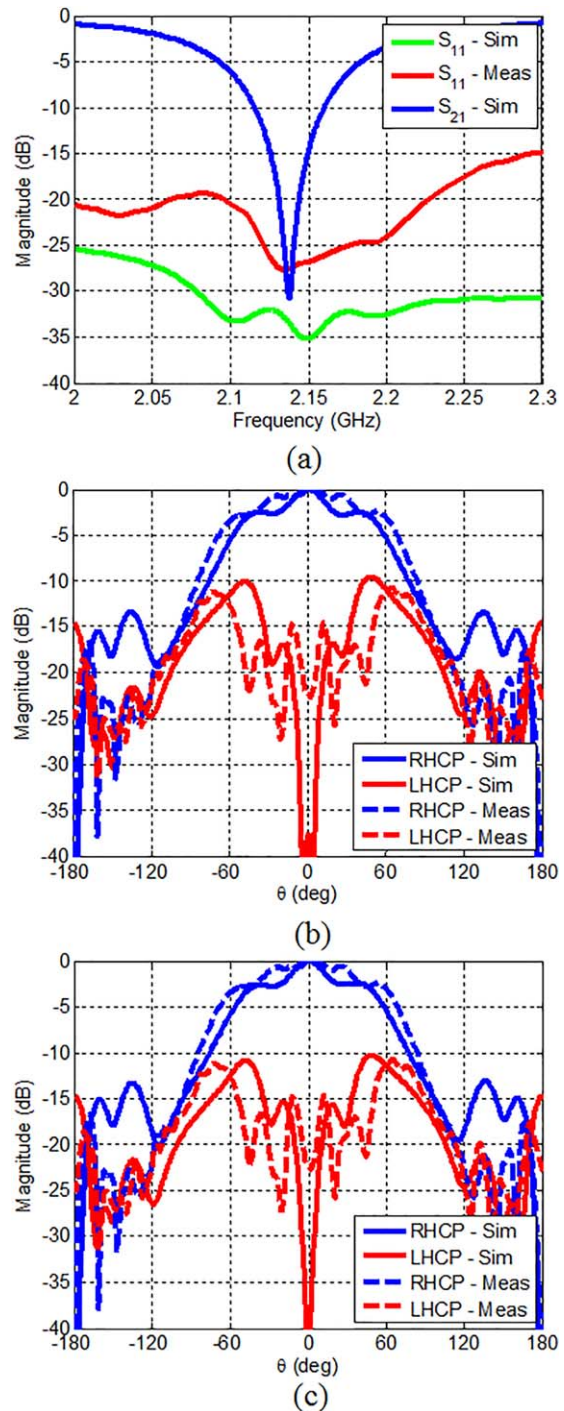


**Figure 1** Circularly polarized square patch antenna used as primary feed. (a)  $S$ -parameters. (b)–(c) Simulated and measured radiation patterns in  $\phi = 0^\circ$  and  $\phi = 90^\circ$  planes, respectively. [Color figure can be viewed at [wileyonlinelibrary.com](http://wileyonlinelibrary.com)]

Refs. [19–22], a LP source was used together with a polarizer to convert linear to circular polarization. Another method based on a LP feed consists in using a high-impedance ground plane together with a PRS that shows a  $90^\circ$  differential phase under two orthogonally incident plane waves [23]. Though both high directivity and circular polarization were achieved, none of the above-mentioned works reduced the overall thickness of the cavity. Using a composite metamaterial surface made of